International Journal of Applied Engineering Research ISSN 0973-4562 Volume 12, Number 12 (2017) pp. 3214-3227

A Study of Tungsten Carbide Surfaces during the Electrical Discharge Machining Using Artificial Neural Network Model

Pichai Janmanee[a]* and Sanya Kumjing[b]

*[a]*Department of Mechanical and Industrial Engineering, Rajamangala University of Technology Krungthep, Bangkok, Thailand.*
[b]*Department of Tool and Die Engineering, Faculty of Engineering and Architecture, Rajamangala University of Technology Suvarnapbumi, Nonthaburi, Thailand.*
**Corresponding Author*

ORCID: 0000-0001-9095-004X

Abstract

In this paper, an artificial neural network (ANN) model was established to predict microcracking during the electrical discharge machining (EDM) of tungsten carbide (WC-Co) composite material using three different electrode materials: graphite, Cu-graphite and Cu-tungsten. The model considered four EDM parameters, such as the electrode material, duty factor, polarity, and discharge current, as feed to the input layer. The microcracks were presented as outputs. The optimal ANN architecture and training algorithm were determined. Comparing the values predicted by the ANN with the experimental data indicated that the trained neural network model provided accurate results. This study shows that the alternative ANN modeling approach can be used to successfully predict microcracking of tungsten carbide during the EDM processes.

Keywords: Artificial neural network, prediction, EDM, microcrack, tungsten carbide, modeling

Nomenclature

EDM = electrical discharge machining

ANN = artificial neural network

WC-Co = tungsten carbide

EDM-3 = graphite

EDM-C3 = Cu-graphite

CTR 08375= Cu-Tungsten

MRR = material removal rate

Cr.Dn = numerical crack density per area

Cr.S.Dn = surface crack density

Cr.Le = mean crack length

N = total number of input factors

w_{ij} = weight of the n^{th} neuron

θ_i = bias or threshold

f(z) = transfer function

z = weighted sum of the inputs

MSE = mean squared error

GM = backpropagation

LM = Levenberg-Marquardt

MPAE = mean absolute percentage error

n = sample size

t = value of the target

R^2 = absolute fraction of variance

O = value of the output

Z_i = weighted sum of the inputs

INTRODUCTION

Electrical discharge machining (EDM) is the process of machining electrically conductive materials by using precisely controlled sparks that occur between an electrode and workpiece immersed in fluid dielectric. The electrode may be considered as the cutting tool. Figure 1 illustrates the basic components of the EDM process [1]. EDM is used in non-traditional manufacturing to develop new technology and manufacture tools that would otherwise be impossible to produce with faster and more conventional methods [2,3]. This machining produces tools with complex-shapes that are used extensively in industries. Furthermore, EDM can be used as a surface finish in the last stage of tool production [4]. Tungsten carbide (WC-Co) with cobalt binder has been widely used as an important tool and die material, mainly because of its high hardness, strength and wear resistance. However, it is difficult to make WC-Co into products with complex shapes and precise dimensions by conventional machining methods [1,5]. The melting point of tungsten carbide is 2,870 °C. Because of its

properties, tungsten carbide cannot be processed easily by conventional machining techniques [5-6]. The EDM process is based on the principle of erosion of materials by electrical sparking. The particles that are removed may be solid, liquid, or gas [7]. Currently, insulating materials can be machined with EDM using an assisting electrode [8]. In the EDM process, copper-tungsten electrodes can be used to produce small holes. Consequently, the process creates opportunities for the machining of tungsten carbide. Tungsten carbide is a type of cemented carbide made by powder metallurgy process, in which the particles of carbide are bound with other metals, such as in tungsten carbide (WC-Co) or titanium carbide (TaC). Tungsten carbide contains very small cobalt particles, 1–10 μm in size, that are used as binders [9]. Microcracks appear on the surface of the tungsten carbide workpiece when they are machined with EDM. Because of their lower melting point, the cobalt particles melt and separate from the tungsten carbide. When using these workpieces as molds or tools, an important problem is their short product shelf life. Singh et al. [10] studied how the electrode material affected the material removal rate (MRR), electrode wear ratio (EWR), surface roughness (SR), and diametral overcut on cutting tool steel grade EN-31. The authors reported that an increase in the current caused an increase in MRR, SR, and diametral overcut. The best-performing electrode was copper, because it showed the maximum material removal rate and the minimum electrode wear ratio, surface roughness, and diametral overcut. Lee and Li [2] researched the effects of the electrode material in the machining of tungsten carbide by comparing copper, graphite, and copper-tungsten electrodes. Copper tungsten had the greatest material removal rate and the lowest electrode wear ratio. As mentioned above, EDM machining is a very complex and stochastic process, in which it is very difficult to determine the parameters for obtaining optimal machining performance. Several researchers have carried out various investigations to model the EDM process using artificial neural networks (ANNs) to predict the characteristics of the surface finish. Some of these studies are discussed below. Tsai and Wang [11] used six different neural network architectures to develop a predictive model for the surface finish in EDM machining, and concluded that there were four models: TANMLP, RBFN, Adaptive RBFN, and ANFIS, which gave consistent results. In addition, Tsai and Wang [12] established and analyzed six neural network models and a neuron-fuzzy model to determine a better process for predicting the MRR. Conversely, a feed-forward neural network with backpropagation learning algorithm was developed by Kao and Tarng [13] to be used in online monitoring of the electrical machining processes. The relationships between tool workpiece gap signals and various pulse types were established, and the ANNs developed could be used to monitor the EDM efficiently. Additionally, Mandal and Pal [14] studied the modeling of the EDM process based on a backpropagation neural network and multi-objective optimization using a non-dominating sorting genetic algorithm. Their experiments were carried out over a wide range of machining conditions for training and verification of the model. The model could predict the response parameters. Markopoulos et al. [15] proposed ANN models for predicting the surface roughness by comparing two well-known programs: MATLAB, with the associated tool boxes, and Netlab. The proposed ANN models could satisfactorily predict the surface roughness and could act as valuable tools for process planning. Koksal [16] reported the prediction of mechanical properties of magnesia-based refractory materials using an artificial neural network. They found no significant differences between the experimental values and ANN results, indicating that the ANN results could be used instead of the experimental values. Azli Yahya et al. [17] studied the model of Artificial Neural Network (ANN) to predict the Material Removal Rate (MRR) during the Electrical Discharge Machining (EDM) process. The ANN model using an input-output pattern of raw data was collected. The experimental data input of copper-electrode and steel-workpiece is based on a selected gap current where pulse on time, pulse off time and the sparking frequency have been chosen. The result significantly demonstrated that the ANN model is capable of predicting the MRR with low percentage prediction error when compared to the experiment result. Somashekhar et al. [18] studied the artificial neural network (ANN) to analyze the material removal of μ-EDM and establish the parameters for optimization of the model. The experiment set up a trained feedforward neural network with back propagation algorithm to optimize the number of neurons and hidden layers to predict a better material removal rate. A neural network model is developed using the MATLAB programming, and the trained neural network is simulated. The experimental results showed that the developed model is within the limits of the agreeable error. Then, genetic algorithms (GAs) were employed to determine the optimum process parameters for any desired output value of the machining characteristics. This well-trained neural network model is shown to be effective in estimating the MRR and is improved using optimized machining parameters. Kumar et al. [19] studied the electric discharge machining process of titanium alloys. The applied artificial neural network coupled with the Taguchi approach was applied for the optimization and prediction of the surface roughness. In the experiment, the analysis migration of different chemical elements and the formation of compounds on the surface were performed using the EDS and the XRD pattern. The results showed that the high discharge energy caused surface defects such as cracks, craters, thick recast layer, micro pores, pin holes, residual stresses and debris. In an EDM operation, it is necessary to select the correct parameters for optimum sparking performance. However, the desired parameters are generally based on experience, instruction manuals or a large number of experimental tests, which require a great amount of time and materials. The objective of the present research is to study the influences of different electrode materials on tungsten carbide workpieces and evaluate the importance of the EDM parameters by developing an ANN models to predict microcracking of the

surface finish during the process. The authors hope that the results of this research can be used to select appropriate parameters and electrode materials in the EDM, mold and tool applications, which will extend the shelf life of tools and eliminate the defective products.

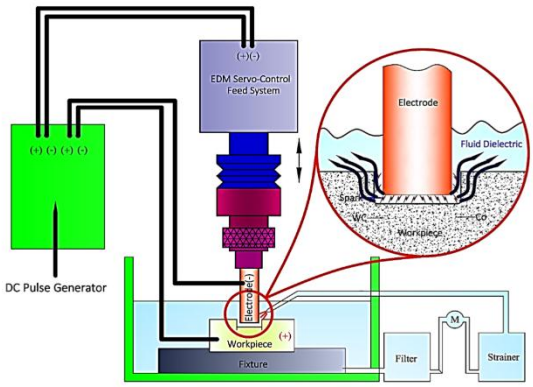

Figure 1. Electrical discharge machining process

EXPERIMENTAL CONDITIONS

To determine suitable parameters for the EDM process, experiments were carried out by varying the following: duty factor, polarity, on time, off time, open circuit voltage, and discharge current. The electrode materials were also varied. The characterization of the products included measurement of the surface microcrack density (Cr.S.Dn). Alongside, suitable EDM parameters were also considered. The workpiece material was tungsten carbide, with a W:Co ratio of 90:10. It was purchased from United Tungsten Co. Ltd, and its properties are shown in Table 1. The EDM conditions used in the experiments are shown in Table 2. The electrodes were 5 mm in diameter, and the depth of the EDM spark was 3 mm. The machine used was numerically controlled (FORM-2-LC, Charmilles Technologies). The electrode materials were Graphite, Cu-Graphite and Cu-Tungsten. Their physical properties are shown in Table 3.

The duty factor, the ratio between the pulse duration and the pulse cycle time, plays an important role in EDM performance. The duty factor is derived from the on-time (time when sparking starts) and off-time (time when sparking stops), according to Equation (1): [3,7].

$$Duty\ Factor\ (\%) = \frac{On-time}{On-time+Off-time} \times 100 \quad (1)$$

,

Where, the units of duty factor are %, the on-time and off-time are in µs, the open circuit voltage is 90 V, and the off-time is 25 µs. To evaluate the surface finish and microcracking, it is important to measure the defects of microcrack on the finished surface of the workpiece after the EDM process. The surface microcrack density on the workpiece may be defined as either: [20-21].

1. Number of microcracks per area (Numerical crack density per area), Cr.Dn (no. of crack/mm^2)

2. Total length of microcracks per area (Surface crack density), Cr.S.Dn (µm/mm^2)

3. Mean crack length, Cr.Le (µm)

In this study, the measurement technique 2 was selected because of the various widths of the samples. The unit used for surface crack density was µm/0.05 mm^2. The Surface Crack Density (Cr.S.Dn) methodology of the workpiece, a measure of the length of Surface Crack Density (Cr.S.Dn) due to the size of the microcracks formed on the surface of the tungsten carbide is very small.

Table 1. Physical properties of tungsten carbide

Properties	Tungsten carbide (WC-Co)
Melting point (°C)	2,870
Density (g/cm^3)	15.7
Thermal expansion (°C)	5×10^{-6}
Hardness (HRA)	87.4
Elastic modulus (GPa)	648
Electrical resistivity (Ω・cm)	17×10^{-6}

Table 2. EDM conditions tested

Duty factor (%)	11, 33, 50, 68, 93
Discharge current (A)	6, 12, 25, 50
Open circuit voltage (V)	90
Polarity (+/-)	+,-
Electrode material	Graphite, Cu-Graphite, and Cu-Tungsten
Workpiece material	Tungsten-Carbide (90% W : 10%Co)
Dielectric fluid	EDM Shell fluid 2A
Flushing	External

Table 3. Physical properties of electrode materials

Properties	Graphite (EDM-3)	Cu-Graphite (EDM-C3)	Cu-Tungsten (CTR 08375)
Melting point (°C)	3,350	1,100	3,500
Density (g/cm^3)	1.81	3.25	15.21
Hardness (HB)	76	67	200
Electrical Resistivity (µΩ.cm)	1400	127	5.5

This makes it difficult to measure using conventional measuring tools. Therefore, it is measured by using a Scanning Electron Microscopy (SEM), which magnifies the image and

makes the microcracks clearly visible. Then, the length and width of the image based on the scale bar is measured as shown in Figure 2. The image goes through the Auto CAD program where the area of the workpiece is measured. The length of is determined by using the command line build onto the microcrack on the surface workpiece, as shown in Figure 3 a). The command to command to check the length of the property line is then used as shown in Figure 3 b). Subsequently, the sum of the length of a microcrack is compared with the scale bar magnification of the image within the measurement results as shown in Table 4.

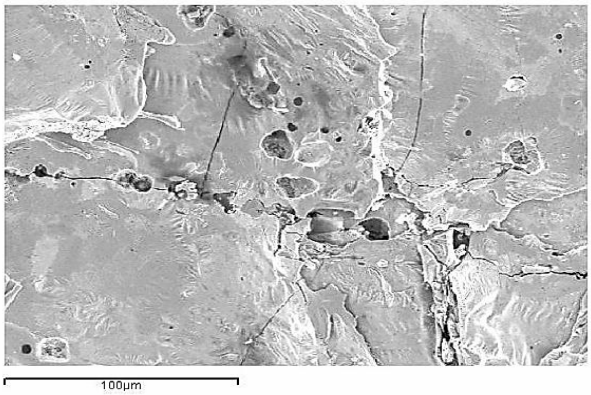

Figure 2. Microcrack on surface tungsten carbide material

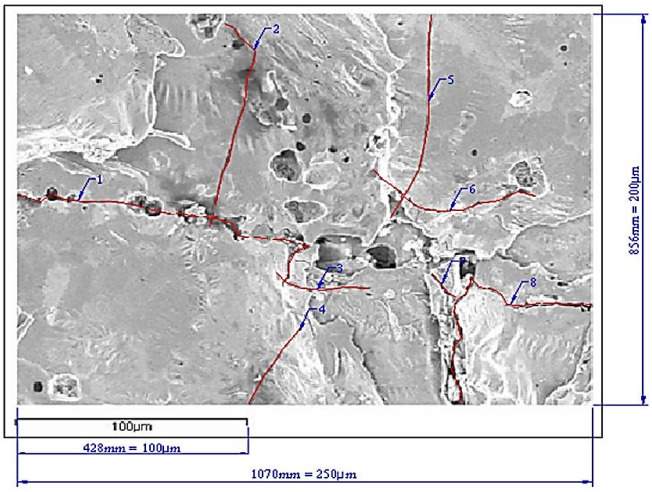

a) Position and micro crack line

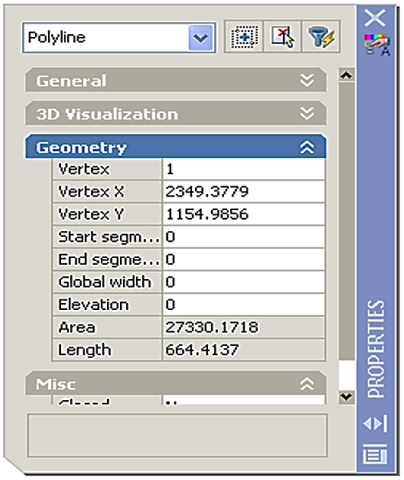

b) Length of microcrack line from Auto CAD program

Figure 3. Surface Crack Density (Cr.S.Dn) methodology of workpiece

Table 4. The example method of Surface Crack Density (Cr.S.Dn)

Positions No.	Micro-crack length from Auto CAD (mm)	Compared with scale bar (µm)
1	664.4137	155.2368
2	436.0246	110.0364
3	171.594	45.3969
4	172.9983	45.7237
5	416.9185	104.0628
6	325.6534	83.0137
7	49.1773	19.5684
8	507.3889	125.6618
Total	2744.1687	688.7005

METHODOLOGY OF ARTIFICIAL NEURAL NETWORK AND MODELING

Artificial neural networks (ANNs) are mathematical representations that replicate the function of a biological network. ANNs are composed of neurons that are used to learn complex functions for solving various applications. The neurons are connected to each other by links known as synapses and associated with each synapse is a weight factor (w). Therefore, a neural network can be trained to find solutions, recognize patterns, classify data and forecast future events. In most cases, an ANN is an adaptive system that changes its structure based on external or internal information that flows through the network during the learning phase. Figure 4 shows a schematic diagram of an artificial neuron. A neuron is a processing unit that forms a weighted sum of input vector components x_1, x_2, …, x_n and transforms this sum by an activation function (also known as a transfer function) $f(z)$ to generate a final output [4], as shown n Equation (2). Neurons may use any differentiable transfer functions such as those

shown in Figure 5. These limit the dynamic range of the input signal and, due to their steep slope, provide high gain for small signals, thus acting as an automatic gain control [15]. In general, the ANN system has three layers: input, hidden, and output. The input layer consists of all the input factors. Information from the input layer is then processed in the course of one hidden layer, followed by the output vector being computed in the output layer as:

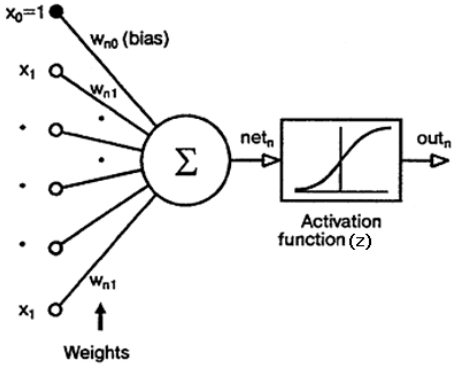

Figure 4. Schematic diagram of an artificial neuron [4]

$$Output = z_n = f\left(\sum_{i=1}^{N} w_{ij} x_j + \theta_i\right), \qquad (2)$$

Where, N is the total number of input factors, w_{ij} are the weights of the nth neuron and θ_i is a bias or threshold. Usually, the bias is interpreted as an extra input, which is set to one (1).

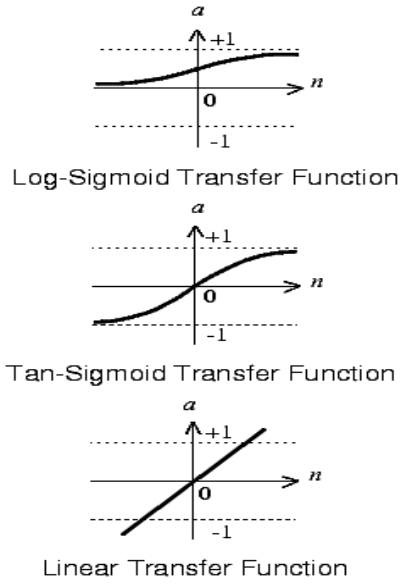

Figure 5. Examples of transfer functions [21]

ANNs are possible candidates for solving problems that have the following characteristics: [4, 22].

- There are sufficient data for network training.
- It is difficult to provide an adequate, simple, and model-based solution.
- New data must be processed at high speed.
- The data processing method needs to be robust to modest levels of noise in the input data.

NEURAL NETWORK MODELING

The modeling of the microcracking behavior in the EDM process was developed using the MATLAB software (MathWorks), along with the neural network toolbox. In this work, the ANN architecture consisted of three layers: input layer, hidden layer, and output [16, 22]. Figure 6 shows a schematic diagram of the neural network architecture used to model the EDM process. The ANN architecture was designed and tested to determine the optimal model for the most suitable prediction.

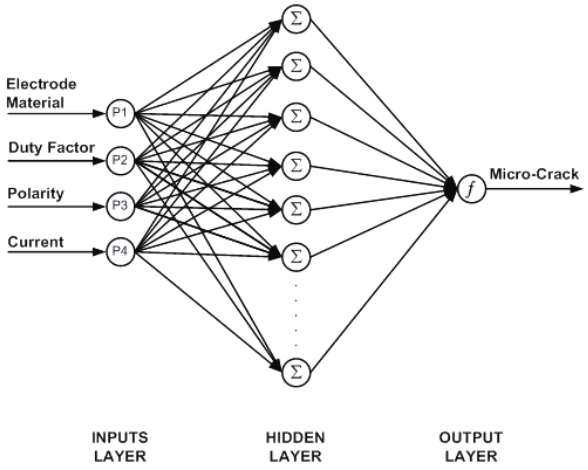

Figure 6. Schematic diagram of neural network architecture used to model the EDM process

The experimental data collated in Table 5 were used for training. Four parameters: electrode material, duty factor, polarity, and current, were fed into the input layers. Because the input data must have suitable numerical values to be used in the program, different types of electrodes were assigned a number: 0 for Graphite, 1 for Cu-Graphite, and 2 for Cu-Tungsten. The positive and negative polarity was assigned 0 and 1, respectively. Then, all the input and target data were normalized so that their mean values were equal to zero and their standard deviations were equal to one. Normalizing data is a technique used with ANNs to avoid reducing the generalization ability and over-fitting. In this study, a multilayer feedforward with an error backpropagation algorithm was used in the training algorithms because of its suitability for solving problems involving function approximations. The hidden layer was improved with numerical optimization techniques, which included the

Levenberg-Marquardt fitting (LM) and scaled conjugate gradient backpropagation (SCG algorithm). This layer was operated upon by a hyperbolic tangent sigmoid transfer and a linear transfer function to give the final layer. The hyperbolic tangent sigmoid transfer function used is shown in Equation (3): [6, 22, 23].

$$f(z) = tanh(z) = \frac{e^{z} - e^{-z}}{e^{z} + e^{-z}}, \quad (3)$$

Where, z is the weighted sum of the inputs.

In this method, the existing data are separated into two sets. The first set consists of three-quarters of the data, which are used to train networks, calculating the gradient and forming the weight factors and bias. The second set contains the remaining randomly selected quarter of the data, used to test the network. After successful training, the system performance is indicated by the mean square error (MSE), according to the Equation (4), and the absolute fraction of variance (R^2) and the mean absolute percentage error (MPAE) are given by the Equations (5) and (6) [6, 23].

$$MSE = \frac{1}{n}\sum_{j}(t_j - O_j)^2 \quad (4)$$

$$R^2 = 1 - \left(\frac{\sum_{j}(t_j - O_j)^2}{\sum_{j}(O_j)^2}\right) \quad (5)$$

$$MPAE = \left(\frac{t - O}{O}\right)x100, \quad (6)$$

Where, n is the sample size, t is the value of the target, and O is the value of the output. The input and output layers are normalized in the range [-1, 1].

RESULTS AND DISCUSSION

The tungsten carbide workpieces sparked with three different electrodes (Graphite, Cu-Graphite, and Cu-Tungsten), duty factor, polarity, and current were analyzed for surface microcrack density (Cr.S.Dn), and the values are listed in Table 5.

Figs. 7–9 show SEM images (magnification 500×) of microcracks on tungsten carbide surfaces after sparking with the positive polarity, using Graphite, Cu-Graphite, and Cu-Tungsten electrodes and duty factors of either 11% or 93%. A high duty factor increased the microcrack density compared with that found by using a low duty factor under similar conditions.

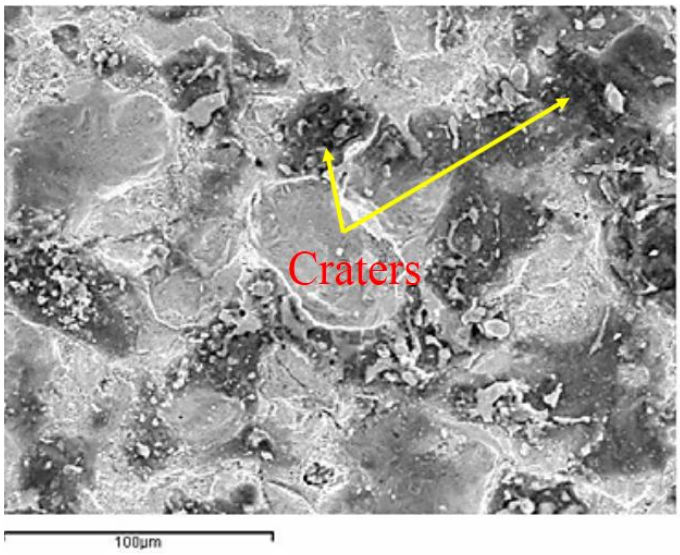

a) Duty factor 11%

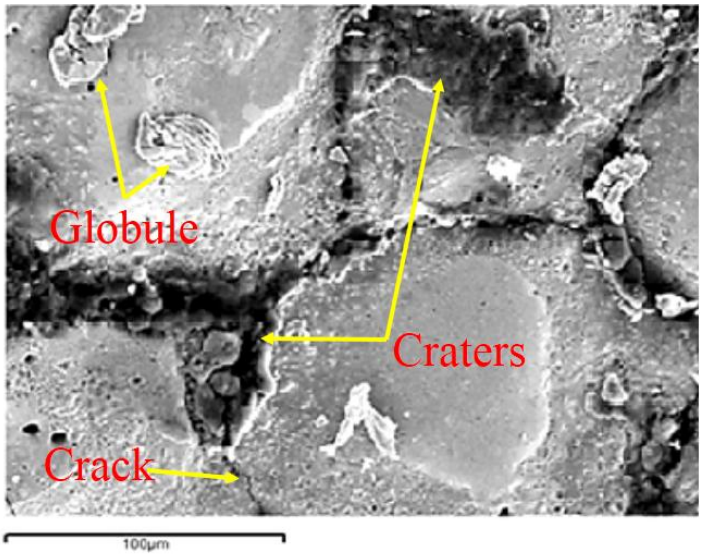

b) Duty factor 93%

Figure 7. SEM images of surface microcracks with graphite electrode, positive polarity, current 6 A, open circuit voltage 90 V.

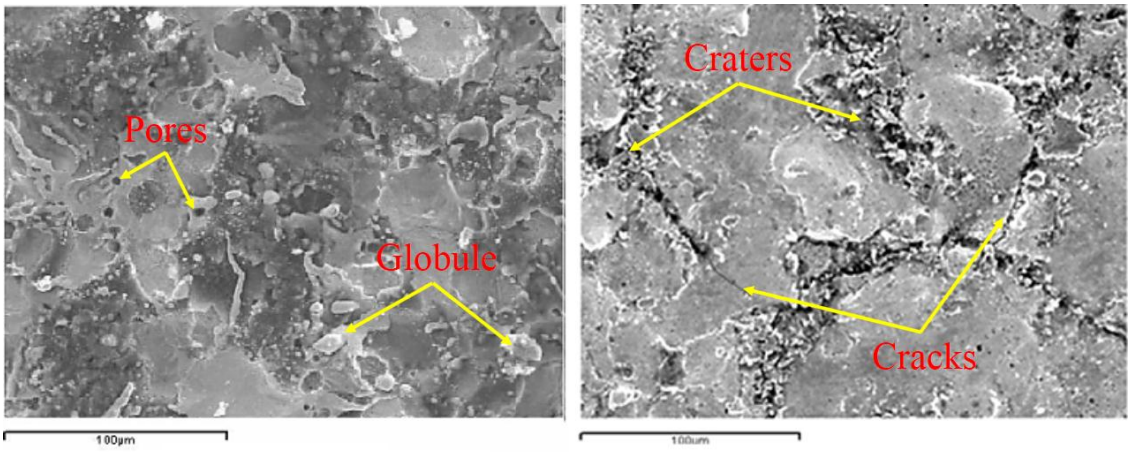

a) Duty factor 11% b) Duty factor 93%

Figure 8. SEM images of surface microcracks with Cu-graphite electrode, positive polarity, current 6 A, open circuit voltage 90 V.

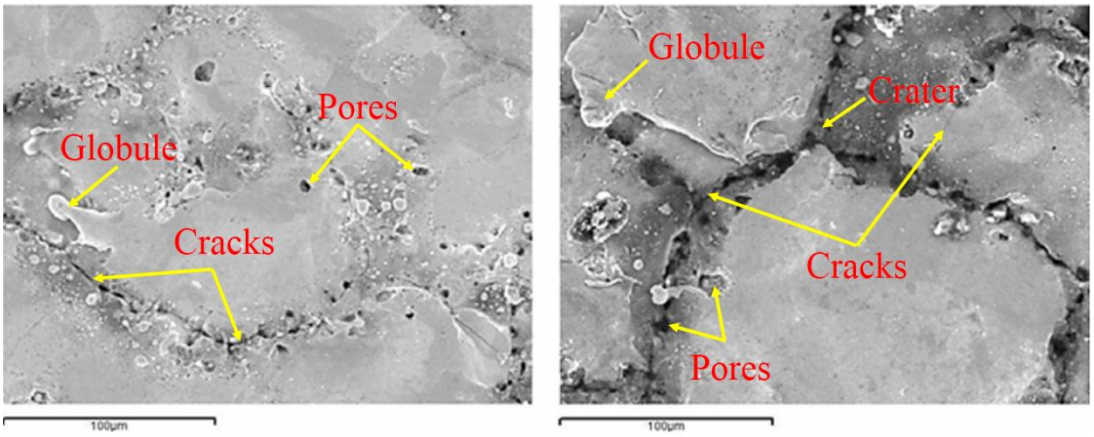

a) Current 6 A b) Current 50 A

Figure 9. SEM images of surface microcracks with Cu-Tungsten electrode, positive polarity, open circuit voltage 90 V duty factor 11%.

Table 5. Experimental conditions and results

Sample No.	Electrode material	Duty factor	Polarity (±)	Current (A)	Cr.S.Dn (µm/0.05mm^2)
1	0	93	0	6	1385.5
2	0	68	0	6	835.5
3	0	50	0	6	735.5
4	0	33	0	6	706.5
5	0	93	1	6	945.2
6	0	68	1	6	598.4
7	0	50	1	6	398.4
8	0	33	1	6	164.5
9	0	11	1	6	83.9
10	0	11	0	6	500.0
11	0	11	0	12	511.3
12	0	11	0	25	1019.4
13	0	11	0	50	1154.8
14	1	93	0	6	1166.1

15	1	68	0	6	858.1
16	1	50	0	6	688.7
17	1	33	0	6	398.4
18	1	93	1	6	1079.0
19	1	68	1	6	903.2
20	1	50	1	6	479.0
21	1	33	1	6	287.1
22	1	11	1	6	188.7
23	1	11	0	6	248.4
24	1	11	0	12	582.3
25	1	11	0	25	948.4
26	1	11	0	50	1014.5
27	2	93	0	6	1153.2
28	2	68	0	6	995.2
29	2	50	0	6	867.7
30	2	33	0	6	708.1
31	2	11	0	6	329.0
32	2	11	0	12	447.0
33	2	11	0	25	872.6
34	2	11	0	50	979.0

Figure7 shows the SEM images of surface microcracks using graphite electrode positive polarity at current 6 A, circuit voltage 90 V, and duty factor is 11% and 93 %, respectively. The experiment result found that the size of the microcrack, pore and craters increase with an increase in the discharge energy level. Moreover, it can be seen that the number of microcracks and globules decreases with an increase in the energy level. In addition, the degree of microcracks increases with an increase in the discharge energy. The large discharge energy causes violent sparks and impulsive force, which strikes the surface workpiece.

The SEM images of the top surface characteristics of the microcracks obtained from the EDM process by using Cu-graphite electrode are shown in Figure 8. The long of on-time from duty factor increase affecting to high energy discharge and produced thickness recast layer and residual stress initiate cracks and any defect such as pores, craters and globules. It can be seen in Figure 7 Figure 8, and Figure 9, respectively.

The SEM images of surface microcracks obtained using the Cu-Tungsten electrode with different discharge currents are shown in Figure 9. Increasing the discharge current increased the microcrack density. However, the experiment result found that a high energy charge during the process produces an inhibitor surface layer carbon on the electrode surface [24]. Thus, an increase in the on-time parameters influence the amount of carbon accumulated at the surface of electrode, which subsequently deacrease the electrode wear. Moreover, the current increase due to high energy discharge causes a large impulsive force, which can remove more debris from the machining gap. Thus, the characteristic of the surface workpiece with high energy discharge can help in reducing the amount of globules on surface [24].

Table 5 presents the details of the parameters used in the study and experimental surface microcrack density results. For each set of parameters, three samples were sparked, the mean values were recorded, and data was collated to be used in the ANN model.

An ANN model was employed to predict the microcracking behavior during the EDM process. The ANN had three layers: an input layer, a hidden layer, and an output layer. In this application, deciding on the number of neurons to use in the hidden layer was the interesting part of the network development process. There is no definite formula for this application. Consequently, a trial-and-error method was used to select the number of neurons in the single hidden layer. Figure10 shows the results of the parametric study conducted to find the optimal ANN model. The relationship between the number of neurons and MSE was determined using a) the SCG Training algorithm, b) the gradient descent with momentum backpropagation (GM) training algorithm, and c) the Levenberg-Marquardt (LM) training algorithm. Figure 10 shows that insignificant changes in the MSE value were found for the GM algorithm using 20 neurons and the LM algorithm using 15 neurons. However, it was clear that 10 neurons in the hidden layer were satisfactory for the SCG algorithm [25-26]. After several network developments in this study, the appropriate ANN structure to predict the microcracking behavior during the EDM process was determined and is presented in Table 6. Figure 11 shows a training error (MSE) curve that indicates the performance of the network during training, with the goal for the training set to 0.005, which ensured a satisfactory response [26-28].

The predictive ability of the ANN model was evaluated based on linear fits between the experimental data and the output of the ANN model, which are presented in Figure 12 and Figure 13. In Figure 12, the blue and red dots represent the training and testing sets, respectively. The linear fit shows very good agreement between the data from the training and testing sets, as indicated by R^2 =0.983, which implies that the ANN model has very high predictive accuracy. The same conclusion can be drawn based on the results and fit in Figure 13. Other statistical error parameter values are shown in Table 7.

Table 8 shows the weight values between the input layer and the hidden layer, which were obtained from the optimal ANN model in Table 6. The activation function used for transferring values between the input and the hidden layer in this study was taken from Equation 5, while Z_i was calculated based on the following Equation 7:

$$Z_i = w_1 \times \text{electrode materials} + w_2 \times \text{duty factor} + w_3 \times \text{polarity} + w_4 \times \text{current} + w5, \quad (7)$$

where Z_i is the weighted sum of the inputs.

Table 6. ANN architecture of optimum network

Number of layers	3
Number of neurons on the layers	Input = 4
	Hidden = 10
	Output = 1
Initial weights and biases	Randomly [-1,1]
Activation functions ; hidden layer; output layer	Hyperbolic -tangent sigmoid Linear
Network training and learning function	SCG algorithm
Adaptive learning rate	0.01
Number of iterations	90
Momentum constant	0.9
Acceptable mean squared error (MSE)	0.005

Table 7. Statistical errors and values

Parameters	Training set	Test set
MSE	0.0042	0.0151
R^2	0.988	0.983
MPE	0.3829	0.8478

Table 8. Weight values between input layer and hidden layer

i	w_1	w_2	w_3	w_4	w_5
1	-0.2976	-1.2404	1.6747	-0.363	2.685
2	-1.2127	-0.4739	1.5827	0.6009	0.9922
3	-1.3848	0.4702	-0.3786	-1.1026	2.6518
4	0.6669	-1.2657	-0.7361	-0.9735	0.8267
5	1.2374	0.886	-1.488	-0.179	0.0499
6	-0.3804	-0.6032	-1.4816	1.1372	-0.6591
7	1.3639	-0.0476	1.6349	0.4346	-0.3592
8	-1.2439	-0.2159	0.5675	-1.2291	-0.1213
9	1.4972	-0.9709	-0.9043	-0.3407	2.8154
10	-0.7171	1.2103	-1.4894	-0.4348	-1.8136

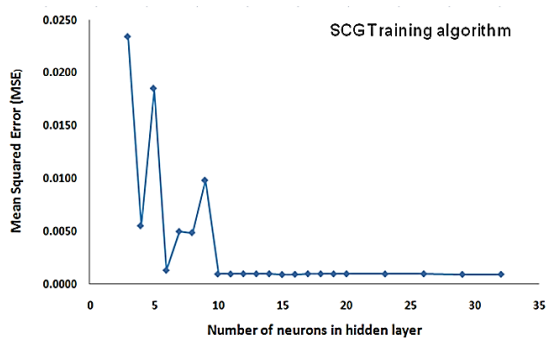

a) SCG Training algorithm

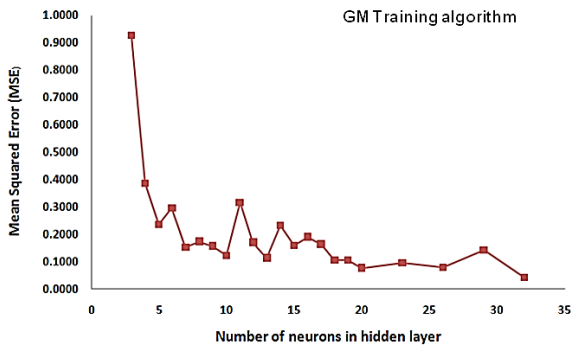

b) GM Training algorithm

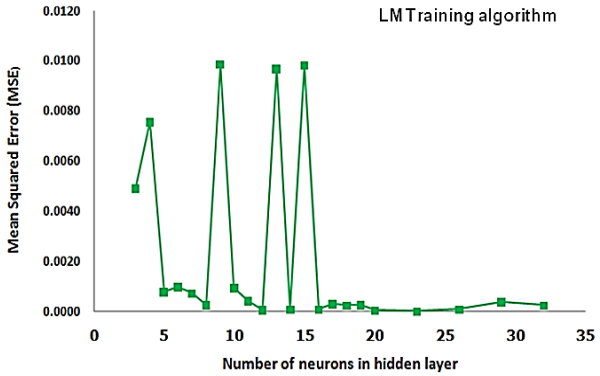

c) LM Training algorithm

Figure 10. Results of the parametric study for determining optimal ANN model.

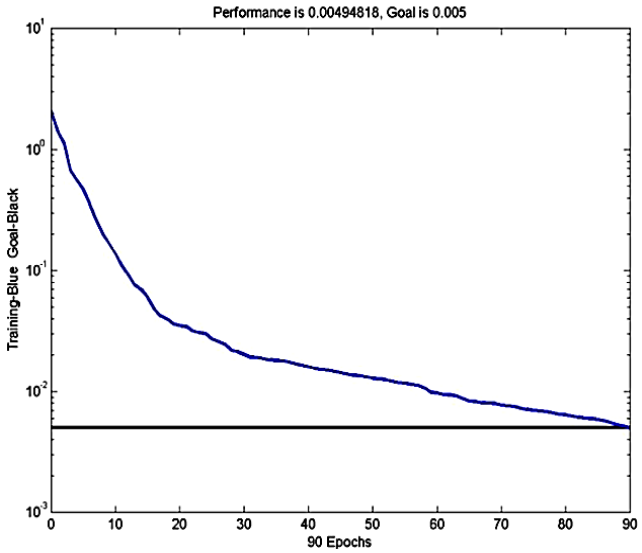

Figure 11. Training error (MSE) curve

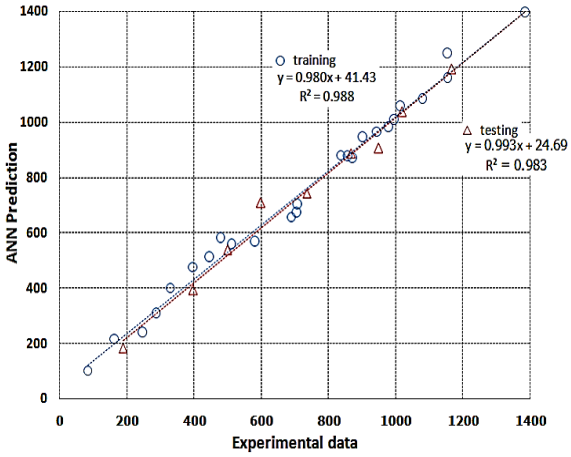

Figure 12. Linear fit between training and testing sets

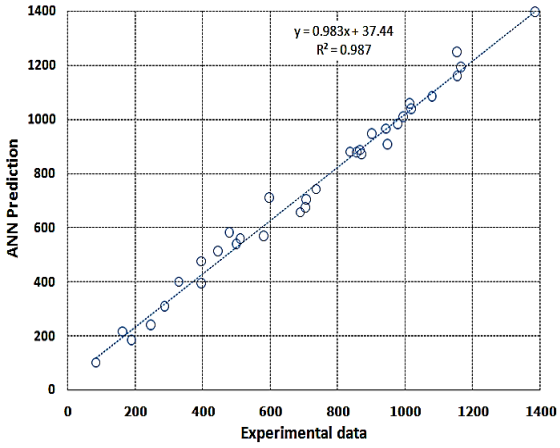

Figure 13. Correlation between experimental data and output of ANN prediction

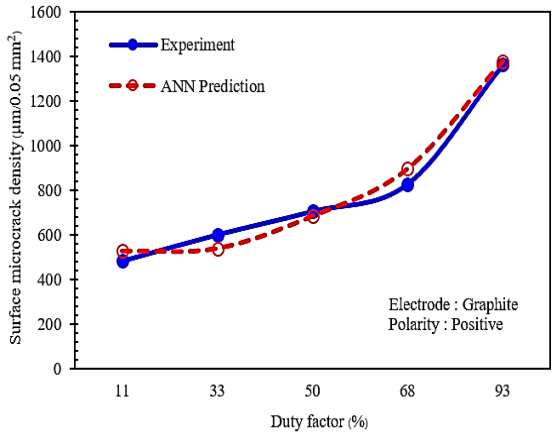

a) Graphite positive polarity

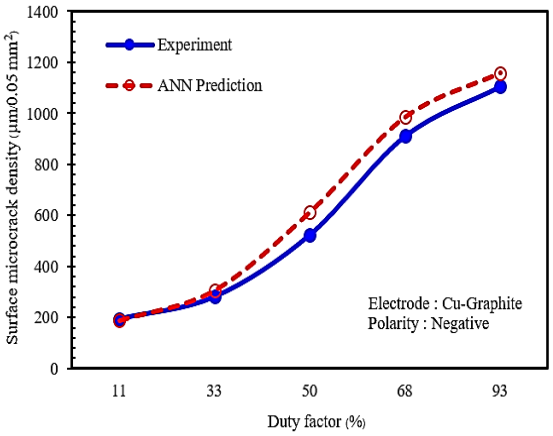

b) Cu-Graphite negative polarity

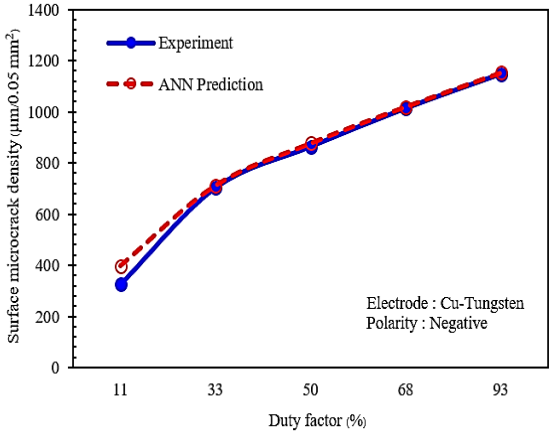

c) Cu-Tungsten negative polarity

Figure 14. Effect of duty factor on surface microcrack density at different electrodes.

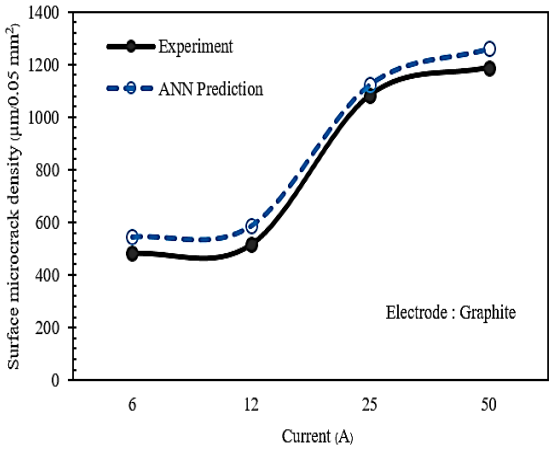

a) Graphite

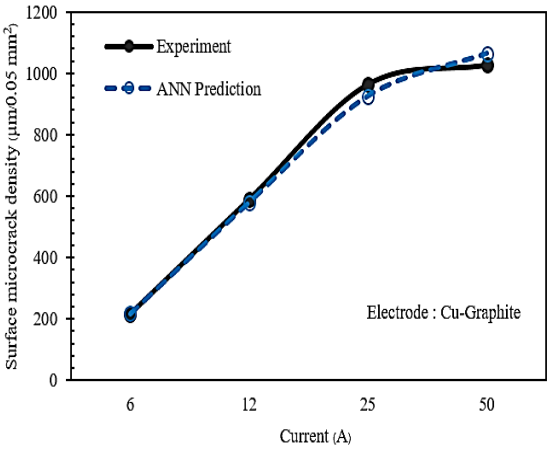

b) Cu-Graphite

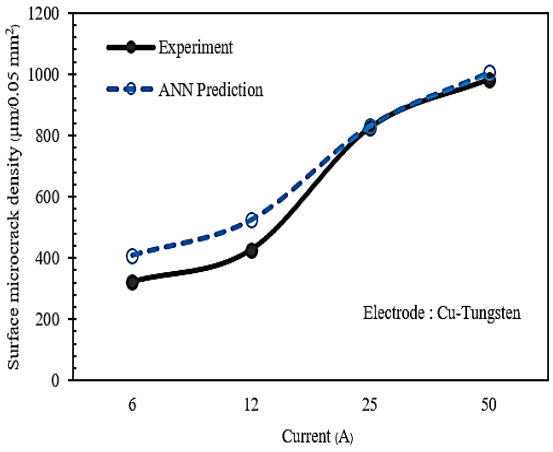

c) Cu-Tungsten

Figure 15. Effect of discharge current on surface microcrack density using different electrodes.

From Equation 7, it was noted that the coefficient w_3 had the largest value of all the input variable weightings and a positive sign, which means that the type of polarity used in the EDM process had a significant effect on the cracking behavior. Positive polarity, according to the results of the experiment shown in Table 5 caused greater microcracking density than negative polarity. In addition, a comparison between the experimental data and ANN predictions in terms of the effect of the duty factor on the surface microcrack density for different electrodes is plotted in Figure 14. The duty factor has a strong influence on the surface cracking in the EDM process, and the predictions from the ANN model were quite close to the experimental results. Figure 15 shows the effect of the discharge current on the surface microcrack density obtained using different electrodes. It was found that higher discharge currents increased surface microcrack density [28], and that the effect was even more significant than that of the duty factor. In other words, the discharge current was the most significant factor affecting microcracking during sparking of a tungsten carbide workpiece.

CONCLUSIONS

In this paper, microcracking on the surface of tungsten carbide workpieces sparked by the EDM process was investigated. The ANN models were then developed to predict the cracking behavior, which depended on EDM parameters such as the electrode material, current, polarity and duty factor. The following conclusions can be drawn from this study:

1) Electrodes Graphite and Cu-Graphite resulted in higher microcrack densities than the electrode Cu-Tungsten. However, during an electric current 6, 12 A microcrack yielded less than the electric current increases. Thus, high energy discharge causes a large impulsive force to surface workpiece and produce to temperature and residual stress, which forms cracks and the residual stress exceeds over the ultimate tensile stress of material.

2) Electrodes with negative polarity led to significantly lower surface microcrack density than electrodes with positive polarity. However, the microcrack density decreased with a reduction in the duty factor and discharge current.

3) In the ANN model, the EDM input parameters, particularly the duty factor and discharge current, had significant effects on the microcrack density of the tungsten carbide workpieces. The discharge current was the most significant factor in microcracking when sparking the tungsten carbide workpiece.

4) The ANN predictions usually harmonized with the experimental values with correlation coefficients (R^2) in the range of 0.983–0.988, mean absolute percentage errors (MPAE) in the range of 0.3829–0.8478%, and very low root mean square errors (MSE).

5) Analyses were carried out to check the adequacy of the artificial neural network (ANN) used for modeling the cracking behavior in the sparked tungsten carbide workpiece. The results indicate that the ANN can predict reasonably accurately.

ACKNOWLEDGEMENTS

The authors are grateful to the Thailand Research Fund, Office of the Higher Education Commission and the National Research Council of Thailand for funding. The authors would like to express their thanks to the National Metal and Materials Technology Center (MTEC) for its kind support in supplying materials and equipment used in this research.

REFERENCES

[1] Guitrau, E. B., "The EDM handbook", Hanser Gardner Publications, pp. 3-19, 1997.

[2] Lee, S.H. and Li, X.P., "Study of the surface integrity of the machined workpiece in the EDM of tungsten carbide", J. Mater. Process. Technol., vol.139, no. 1-3, pp. 315-321, 2003.

[3] Mahdavinejad, R.A. and Mahdavinejad, A., "ED machining of WC-Co", J. Mater. Process. Technol., vol. 162-163, pp. 637-643, 2005.

[4] Shtrauss, V. and Lomanovskis, U., "Structural evaluation of materials by artificial neural networks", Mechanics of Composite Materials, vol. 35, no. 1, pp. 77-88, 1999.

[5] Song K.Y., Chung D.K., Park M.S, and Chu C.N., "Water spray electrical discharge drilling of WC-C", International Journal of Precision Engineering and Manufacturing, vol.13, no 7, pp. 1117-1123, 2012.

[6] Nagesh, D.S. and Data, G.L., "Prediction of weld bead geometry and penetration in shielded metal arc welding using artificial neural networks", J. Mater. Process. Technol., vol. 123, no. 2, pp.303-312, 2002.

[7] Ho, K.H. and Newman, S.T., "State of the art electrical discharge machine (EDM)", International Journal of Machine Tools & Manufacture, vol. 431, pp. 287-1300, 2003.

[8] Muttamara, A., Fukuzawa, Y., Mohri, N. and Tani T., "Probability of precision micro-machining of insulating Si_3N_4 ceramics by EDM", J. Mater. Process. Technol., vol. 140, no. 1-3, pp. 243-247, 2003.

[9] Puertas, I., Luis C.J. and Alvarez, L., "Analysis of the influence of EDM parameters on surface quality: MRR and EW of WC-Co", J. Mater. Process. Technol., vol. 153-154, pp. 1026-1032, 2004.

[10] Singh, S., Maheshwari, S. and Panday P.C., "Some investigation into the electric discharge machining of hardened tool steel using different materials", J. Mater. Process. Technol., vol. 149, no. 1-3, pp. 272-277, 2004.

[11] Tsai, K.M. and Wang P.J., "Comparisons of neural network models on material removal rate in electrical discharge machining", J. Mater. Process. Technol., vol. 117, no. 1-2, pp. 111-124, 2001.

[12] Tsai, K.M. and Wang, P.J., "Prediction on surface finish in electrical discharge machining based upon neural network models", International Journal of Machine Tools & Manufacture, vol. 41, no. 10, pp. 1385-1403, 2001.

[13] Kao J.Y. and Tarng, Y.S., "A neural network approach for the on- line monitoring of the electrical discharge machining process", J. Mater. Process. Technol., vol. 69, no. 1-3, pp. 112-119, 1997.

[14] Mandal, D. and Pal, S.K., "Modeling of electrical discharge machining process using back propagation neural network and multi-objective optimization using non-dominating sorting genetic algorithm-II", J. Mater. Process. Technol., vol. 186, no. 1-3, pp.154-162, 2007.

[15] Markopoulos, A.P., Manolakos, D.E. and Vaxevanidis, N.M., "Artificial neural network models for the prediction of surface roughness in electrical discharge machining", Journal of Intelligent., vol.19, Issue 3, pp. 283-292, 2008.

[16] Koksal, N.S., "Prediction of mechanical properties in magnesia based refractory materials using ANN", Computational Materials Science, vol. 47, no. 1, pp. 86-92, 2009.

[17] A. Yahya., T. Andromeda, A. Baharom, A.A. Rahim and N. Mahmud., "Material Removal Rate Prediction of Electrical Discharge Machining Process Using Artificial Neural Network", Journal of Mechanics Engineering and Automation. vol.1, pp. 298-302, 2011.

[18] K. P. Somashekhar., N. Ramachandran and Jose Mathew., "Optimization of Material Removal Rate in Micro-EDM Using Artificial Neural Network and Genetic Algorithms", Materials and Manufacturing Process, vol. 25, pp. 467-475, 2010.

[19] Kumar, S., Batish, A. Singh, R. and Singh T. P, "A hybrid Taguchi-artificial neural network approach to predict surface roughness during electric discharge machining of titanium alloys", Journal of Mechanical Sci. and Technol., vol.28 (7), pp. 2831-2844, 2014.

[20] O'Brien, F.J., Taylor, D. and Lee T.C., "Microcrack accumulation at different intervals during fatigue testing of compact bone", Journal of Biomechanics, vol. 36, no. 7, pp. 973-980, 2003.

[21] N. Surtragul, "Effect of electrode on micro-cracks of EDMed tungsten carbide", The Degree of Master of Engineering (Industrial Engineering), Faculty of Engineering, Thammasat University, 2008.

[22] Gupta, A.K., Singh, S.K., Swathi, M. and Gokul, H., "Prediction of flow stress in dynamic strain ageing regime of austenitic stainless steel 316 using artificial neural network", Mater. Des., vol. 35, pp. 589-595, 2012.

[23] Vasudevan, M., Bhaduri, A.K., Raj, B. and Rao, K.P., "Delta ferrite prediction in stainless steel welds using neural network analysis and comparison with other prediction methods", J. Mater. Process. Technol., vol. 142, o. 1, pp. 20-28, 2003.

[24] M.D Ashikur Rahman Khan, M.M. Rahman, and K.

Kadirgama. "Neural Network Modeling and analysis for surface characteristics in electrical discharge machining", 10th International Conference on Mechanical Engineering, ICME 2013. Procedia Engineering, vol. 90, pp. 631-636, 2014.

[25] G. Krishna Mohana Rao G., Rangajanardhaa, D. Hanumantha Rao and M. Sreenivasa Rao., "Development of hybrid model and optimization of surface roughness in electric discharge machining using artificial neural networks and genetic algorithm", J. Mater. Process. Technol., vol. 209, pp.1512–1520, 2009.

[26] M.A.R. Khan, M.M. Rahman, K. Kadirgama, R.A. Bakar, "Artificial neural network model for material removal rate of Ti-15-3 in electrical discharge machining", Energy Edu. Sci. Tech. Part A: Energy Sci. Res., vol. 29, no.2, pp.1025–1038, 2012.

[27] M.A.R. Khan, M.M. Rahman, K. Kadirgama, M.A. Maleque, R.A. Bakar, "Artificial Intelligence Model to Predict Surface Roughness of Ti-15-3 Alloy in EDM Process", World Acad. Sci. Eng. Tech. vol.74, pp.121–125, 2011.

[28] W. Daosud, K. Jariyaboon, P. Kittisupakorn, and M. Azlan Hussain, "Application of Neural Network in the System of Self-Diagnosis-Car", International Journal of Applied Engineering Research. vol. 12, no. 2, pp. 246–248, 2017.